mathematics

MDPI

Article

Influence of Transfer Epidemiological Processes on the Formation of Endemic Equilibria in the Extended SEIS Model

Alexander R. Karimov [1,2,*], Michael A. Solomatin [2] and Alexey N. Bocharov [1]

[1] Joint Institute for High Temperatures, Russian Academy of Sciences, Izhorskaya St. 13 Bd.2, Moscow 125412, Russia; bocharov.ya@yandex.ru
[2] Department of Electrophysical Installations, Institute of Nuclear Physics, National Research Nuclear University MEPhI, Kashirskoye Shosse 31, Moscow 115409, Russia; mis4455@yandex.ru
* Correspondence: arkarimov@mephi.ru

Abstract: In the present paper, a modification of the standard mean-field model is considered, allowing for the description of the formation of a dynamic equilibrium between infected and recovered persons in a population of constant size. The key point of this model is that it highlights two-infection transfer mechanisms depending on the physical nature of the contact between people. We separate the transfer mechanism related directly to the movement of people (the so-called transport processes) from the one occurring at zero relative speed of persons (the so-called social contacts). Under the framework of a physical chemical analogy, the dependencies for the infection transfer rate constants are proposed for both purely transport and social mechanisms of spread. These dependencies are used in discussing the formation of quasi-stationary states in the model, which can be interpreted as endemic equilibrium states. The stability of such endemic equilibria is studied by the method of Lyapunov function.

Keywords: SEIR model; endemic equilibrium; infection transmission rate constant; Lyapunov function

MSC: 92D30

Citation: Karimov, A.R.; Solomatin, M.A.; Bocharov, A.N. Influence of Transfer Epidemiological Processes on the Formation of Endemic Equilibria in the Extended SEIS Model. *Mathematics* **2024**, *12*, 3585. https://doi.org/10.3390/math12223585

Academic Editors: James P. Braselton and Martha L. Abell

Received: 29 October 2024
Revised: 11 November 2024
Accepted: 12 November 2024
Published: 15 November 2024

1. Introduction

In the present work, the modification of the standard SEIR model for the spread of infectious diseases [1–5] was used to study the formation of dynamic equilibrium between infected and recovered persons in a population of constant size under the influence of external and intra-population factors. In the present paper, we used a model called the "SEIS model" since we excluded from consideration fully recovered persons who may be immune to the disease in question. From a medical point of view, such a type of equilibrium, when the population simultaneously acts as a source and environment for disease development, may be treated as some form of endemicity [1,5]. In this case, there is a category of persons who, being carriers of the virus, do not yet show obvious symptoms of the disease and are in the latent phase of the disease. A typical example of such a disease can be tuberculosis [6,7], which, despite enormous efforts to eradicate it, remains an inevitable attribute of modern society. This example highlights the importance of identifying the role of such a hidden factor in the development of infectious diseases.

It should be expected that both the transition to an epidemic and the disappearance of the disease in such a population are possible. The implementation of the disease development scenario is mainly determined by the ratio of the constants for the corresponding epidemiological transitions determining the transmission of the infection (see, for example, [2,3,8–10]). Therefore, determining dependences for the epidemiological constants of a different nature is a key point for establishing the infection transfer mechanism and achieving endemic equilibrium in the population.

The formal similarity between equations of epidemiological mean-field models [1,5] and chemical kinetics allows us to establish such dependencies based on a physical kinetics approach that has been used for determining the rate constants of chemical reactions (see, for example, [11] and the references therein). In the framework of such an analogy, one can assume that some epidemiological constants may be represented in a form analogous to the Arrhenius formulas, which determine the rate of chemical reactions. However, in these epidemiological dependencies, the role of temperature will be played by some physical factors characterizing the population as a whole, for example, the average distance between people—a.

In the framework of the modified SEIR model, we worked out such an analogy for estimating the epidemiological constants that are responsible for the transmission of the infection. In this way, it would be of interest to examine what new endemic states emerge in such modified mean-field models due to the influence of these epidemiological constants. Also, it is of interest to discuss the stability of these states.

2. Formulation of the Endemic Problem

To modify the SEIR model equations for a closed population of a constant size (i.e., without considering birth, death, and migration processes), we will adjust part of the equations [1–5] to explicitly highlight the transmission of the infection across persons who are in the symptomatic stage of the disease and from people who have just been infected (so-called latent sick persons). One can assume that the transmission of infection for each category of people comes about in different ways, and these processes are characterized by different rate constants of infection transmission. Indeed, the latent sick persons often interact with other people during their movements, while those who have been symptomatic for some time tend to have contacts limited to their immediate surroundings. Moreover, unlike the standard SEIR model, we disregarded the group of persons with either innate immunity or acquired immunity post-recovery. This means that recovered persons can be re-infected.

In this case, the main SEIS model equations, expressed in terms of the specific proportions of infected and healthy persons, can be reduced to the following:

$$\frac{dS}{dt} = -(\beta_I SI + \beta_E SE) + \gamma I + \alpha E, \tag{1}$$

$$\frac{dE}{dt} = \beta_I SI + \beta_E SE - (\delta + \alpha)E, \tag{2}$$

$$\frac{dI}{dt} = \delta E - \gamma I, \tag{3}$$

where S is the proportion of susceptible persons in the population at the current time t (i.e., uninfected persons; in fact, this is the group of healthy people), E is the proportion of exposed persons (i.e., persons already infected but not yet sick; in fact, this is the latent group), and I is the proportion of infectious persons (i.e., individuals who are sick at the current time t). The constant β_I describes the transmission rate of the virus from sick persons to the healthy persons, β_E characterizes the transmission of the disease from infected persons, γ is the constant characterizing the rate of transition from the group of sick persons to healthy individuals, α is the constant for the transition from the latent group to the category of healthy persons, and δ is the constant rate for the transition from infected to the group of sick persons.

It is worth noting that the system of (1)–(3) automatically ensures the constancy of the population under consideration:

$$S + E + I = 1 \tag{4}$$

for any moment of time $t \geq 0$.

For the system of (1)–(3), we shall consider the Cauchy problem; that is, there is initially some number of infected and sick persons in the population. The initial proportions are assumed to be such functions as follows:

$$S(t=0) = S_0 > 0, E(t=0) = E_0 \geq 0,\ I(t=0) = I_0 \geq 0, \tag{5}$$

that the conditions (4) must be fulfilled. In this case, the epidemiological constants β_E and β_I are treated as some governing parameters defining the system's evolution.

It should be noted that the assumption of a constant population size shall be acceptable if the average duration of a disease in the considered population is sufficiently short compared to the average time of generational change. Such an approximation shall also be acceptable in the case where the birth rate is approximately equal to the death rate. That is a natural restriction for the SEIS model worked out, which leaves many diseases out of consideration that have existed in the population for many years. Therefore, it is also necessary to consider models where demographic processes would be taken into account explicitly. We hope to discuss these questions in our forthcoming works.

3. Basic Epidemiological Constants

First of all, we established the allowable range for the values of β_E and β_I proceeding from the point that in the order of magnitude, they must coincide with the similar constant β used in the standard SEIR model. According to [12–14], the value of the constant β lies in the range of 0.1 to 1.5 days^{-1}, regardless of the type of infection: for the seasonal flu, this value can range from 0.3 to 1.5 days^{-1} [15–17]; for the COVID-19 pandemic, the characteristic value of β is in the range of 0.1–0.5 days^{-1} [18–20]. Although it looks like the value of β weakly depends on the nature of the virus, in reality, the rate of infection transmission mainly depends on the type of virus and the contact rate within the population. Nevertheless, for sufficiently close types of pathogens, in a first approximation, β_E and β_I may be assumed to be independent of the nature of the infection and the individual medical–biological characteristics of people by considering only the influence of the physical and social conditions in which the population under consideration is located. That is, in the present work, we only focused on the contact rate within the population.

So, we tried to explicitly establish such a dependence for the infection transmission rate constants β_l, here, $l = E,\ I$, on the gas–kinetic parameters of aerosols, which are an integral part of human respiration, as well as the average distance between persons for a well-mixed population of constant size, where it is not necessary to separate the contacts of infected from healthy persons. In this case, the virus transmission rate β_l in Equations (1)–(3) is determined by the product of the average number of contacts ν_l for category l per unit time, capable of leading to infection transmission (in essence, this value is analogous to the collision frequency in physical kinetics), and the probability of infection transmission w in a given contact:

$$\beta_l = \nu_l w. \tag{6}$$

Here, we assume that the probability of infection transmission is the same for all categories of infection carriers. That is, here, the distinctions in β_E and β_I arise due to the different nature of the contact frequency ν_l. However, this is a purely physical point of view; in reality, one should take into account some socio-cultural factors that determine possible routes of infection transmission [21]. We briefly will touch on these points in Section 8.

To determine the value of w, we proceeded from the point that the infection is spread only by aerosol particles during human breathing, and an infectious contact was defined as a healthy person entering a certain zone around an infected person. The characteristic volume of this area is assumed to be the volume of a cone (see Figure 1) with a height l_x and a cross-sectional area $\sigma_{ep} = \pi l_y^2$, $V_{ep} = \pi l_x l_y^2/3 \approx l_x l_y^2$, where l_x is the distance that an exhaled aerosol particle can travel horizontally relative to the ground surface, and l_y is the distance that this particle can move vertically under the influence of gravity. The dependence of l_x and l_y on the characteristics of aerosol particles and environmental

conditions was discussed in [22,23]. These studies showed that, depending on the weight of the aerosol particle and the Reynolds number, l_x varies within $0.2 \leq l_x \leq 2$ m, and the maximum vertical displacement l_y is around 2 m. These spatial measures shall be used later in evaluating w.

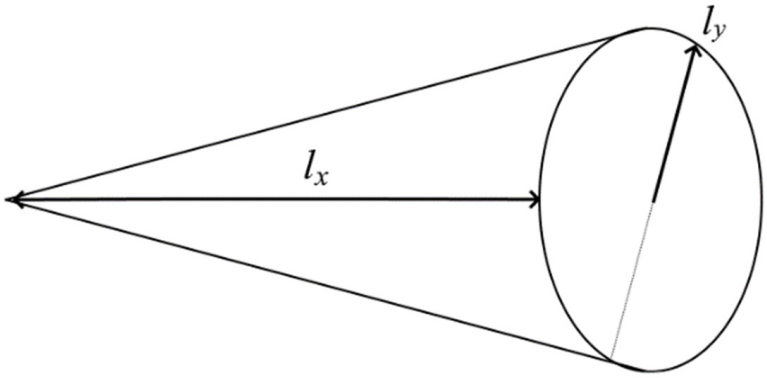

Figure 1. Effective volume of infection.

Knowing the value of a, by analogy with the Loschmidt number [24,25], we can calculate the characteristic volume per person and hence estimate the characteristic density of people in the considered population as $n = a^{-3}$. This allows us to make a rude estimation for the characteristic volume occupied by the entire population as $V_{pl} = N/n = Na^3$. Here, N is the number of persons in the taken population (it is worth noting that $1 \ll N < \infty$). So, the probability of infection is V_{ep}/V_{pl} for a person entering into the volume V_{ep}. Herewith, the probability of remaining healthy for this person is $1 - V_{ep}/V_{pl}$. Then the probability of not becoming infected from this volume for N people is estimated as follows:

$$p(a, l_x, l_y) = \left(1 - V_{ep}/V_{pl}\right)^N = \left(1 - \frac{l_x l_y^2}{Na^3}\right)^N. \tag{7}$$

For $N \gg 1$, this relation reduces into the following:

$$p(a, l_x, l_y) = \lim_{N\to\infty}\left(1 - \frac{l_x l_y^2}{Na^3}\right)^N = \exp\left(-\frac{l_x l_y^2}{a^3}\right), \tag{8}$$

Using this value, we arrive at the following estimate for the full probability of infection by the effective volume:

$$w = 1 - p = 1 - exp\left(-\frac{l_x l_y^2}{a^3}\right) \tag{9}$$

It is worth noting that this expression describes a physically reasonable dependence for the infection probability on the parameters a, l_x, and l_y. Indeed, in the limit of (1) $a \to 0$ and $l_x, l_y \to \infty$, we have $w \to 1$, whereas in the case of (2) $a \to \infty$ and l_x, $l_y \to 0$, we obtain $w \to 0$. For $l_x, l_y \ll a$, the relation (9) is reduced to the following:

$$w = \frac{l_x l_y^2}{a^3}. \tag{10}$$

As is seen from the present relation, in this case, the probability of infection is proportional to the effective infection volume and inversely proportional to the volume per person.

We now move on to the discussion of the contact frequency ν_l. In principle, this value may have both a transport and a social component and we can write it as follows:

$$\nu_l = \zeta_l \nu_{sc} + \xi_l \nu_{tr}, \tag{11}$$

where ν_{tr} is the transport frequency, which is due to the mutual movement of people relative to each other, and ν_{sc} is the frequency of social contacts, which is not directly related to people's movement. That is, ν_{sc} should be understood as those contacts between people that do not require movement, for example, a group of people sitting together in some public place (e.g., transport or conference). Also, we introduced two coefficients, ζ_l and ξ_l, to take into account the specific contribution of the considered type of contact to the total frequency ν_l. It is clear that the choice of these factors requires a detailed analysis of transport and social processes. However, while this question emerges from the framework of the present paper, we hope to discuss this point later. Therefore, as an illustration, here we shall limit ourselves to the case when these parameters can take values of either zero or one.

Thus, the relationship between (6), (9) and (11) can be used to describe the theoretical dependence of the infection transmission rate on external factors. Here, the other epidemiological constants α, γ and δ mainly depend on medical and biological factors, and environmental characteristics apparently do not directly influence these ones. However, these constants are required in order to study the model of (1)–(3), so we will briefly delve into these ones.

So, the value of the constant δ is estimated based on the average incubation period τ_{inc} [25–27] that is considered as a time between the moment of infection and the onset of symptoms in an infected person, i.e., one can use $\delta = 1/\tau_{inc}$. It seems that this characteristic is determined by the biological features of individual people. Observations show that the typical values of τ_{inc} lay in the range from 3 to 5 days [28]. In a similar way, the magnitudes of γ and α are estimated. According to [29], the average duration of the infectious period τ_{inf} ranges from 3 to 14 days, and we have $\gamma = 1/\tau_{inf}$. Recall that the constant coefficient α has been introduced into the model in order to respond to the transition from the group of the exposed patients to the category of susceptible persons. In fact, the epidemiological constants α and δ describe similar processes: the transition from a given group to the category of sick or healthy. In this case, one can expect that values of these constants are the same in order of magnitude. It is this property that we shall explain further when choosing the values of the constants α and δ.

From this consideration, it follows that there are realistic scripta where the epidemiological constants α, γ and δ remain constant over a long period of time, whereas β_E and β_I depend on environmental and population characteristics, hence these constants can vary within a wide range, which inevitably should affect the establishment of an equilibrium in the system under consideration. Therefore, it is worth discussing in more detail the dependence of the constants of transportation and social transmission rates of infections on external conditions.

4. Transportation Mechanism of Infection Transfer

Formula (11) with $\zeta_E = 0$ and $\xi_E = 1$ describes the transfer of infection solely due to the mutual movement of people relative to each other. As an estimate for ν_{tr}, one can take the value that is the inverse of the time it takes to traverse the distance between people, i.e., one can use the following:

$$\nu_{tr} = \frac{U_{tr}}{a}, \tag{12}$$

where U_{tr} is the average velocity of a person.

Here, to simplify the analysis, we relaxed the impact of the discreteness of breathing on the spread of infection: the flow of exhaled air is assumed to be constant for the following reason. As is known, the breathing process is characterized by the frequency of breathing movements ν_{tr}. In a healthy person, this value is $16 \leq \nu_{br} \leq 20$ breaths per minute;

therefore, we can estimate the duration of one breathing movement to be $16 \leq \tau_{br} \leq 20$ s. Clearly, if $\tau_{br}\nu_{tr} \ll 1$, we may neglect the finite time of breathing movement, and this case is fulfilled under normal conditions.

Then substituting (9) and (12) into (6), we arrive at the following:

$$\beta_E = \nu_{tr} w = \frac{U_{tr}}{a}\left[1 - exp\left(-\frac{l_x l_y^2}{a^3}\right)\right], \tag{13}$$

As is seen from this relationship, when,

$$l_x l_y^2 / a^3 \ \leq 1, \tag{14}$$

then the magnitude of β_E is most strongly affected by the distance between people a and the average movement velocity U_{tr}.

In order to fully display the character of this dependence, we performed some estimations for typical real conditions by using some empirical information. As a rule, a person takes an average of 6000–10,000 steps per day over 6–12 h [30] (with a step length of 0.8 m). Proceeding from this point, we found that $U_{tr} = 0.4 \div 1$ m/s. Since β_E linearly depends on U_{tr}, we limited our consideration to the dependence $\beta_E = \beta_E(a)$ for a permissible l_x and l_y only for $U_{tr} = 1$ m/s.

Figure 2 presents the dependence for β_E as a function of the distance between people a for different values of l_x and l_y. As is seen from this figure, for a large $a > 5$ m, the value of the β_E constant becomes negligible ($\beta_E \ \leq 10^{-2}$ s^{-1}). However, the most interesting results are observed in the region of small distances ($a < 1$ m), where the dependence of $\beta_E(a)$ has a hyperbolic character, and there is a strong influence of l_x and l_y on the value of β_E.

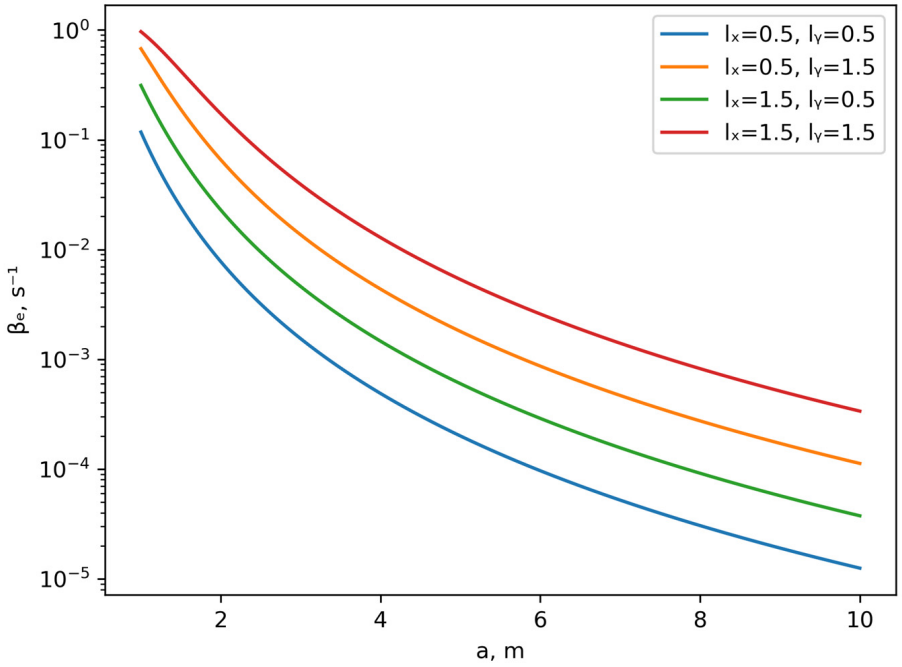

Figure 2. Dependence of β_E on the average distance between people α for different l_x and l_y values at $U_{tr} = 1$ m/s (here, l_x and l_y are measured in meters).

Since under normal conditions, $\nu_{tr} \gg \nu_{sc}$, the infection transmission rate should mainly be determined by Equation (13). Therefore, it is of interest to compare the present theoretical dependence with the relevant empirical data on the infection transmission rate constant β used in the standard SEIR model for large cities taking into account the average distances between people in these cities.

To produce such an analysis, we used the information on the COVID-19 epidemic modeled in Moscow, Berlin, New York, and Paris [31–36]. The characteristic values of a for the chosen cities was estimated based on the corresponding demographic data for the population density of these cities by using the relation $a = 1/\sqrt{n}$, where the population density n is calculated in the number of people per square meter (noting that here we have again applied the analogy with the Loschmidt number). The corresponding values for a are represented in Table 1.

Table 1. The characteristic values of a for different cities.

City	Population Density, $person/m^2$	Distance between People, m
Berlin	0.004	15.7
Moscow	0.005	14.1
London	0.0057	13.4
New York	0.0107	9.6

In order to make this comparison complete, we had to also take into account the influence of U_{tr}, l_x, and l_y in the chosen cities [see Equation (13)]. However, this requires detailed information about such governing parameters. We shall bypass this point considering the set of curves β_E(a) for physical permissible parameters.

The corresponding theoretical dependencies and empirical points are shown in Figures 2 and 3. As is seen from these graphs, the theoretical dependence in Equation (13) for the chosen range of the governing parameters in an acceptable manner coincides with the experimental data (see Figures 3 and 4).

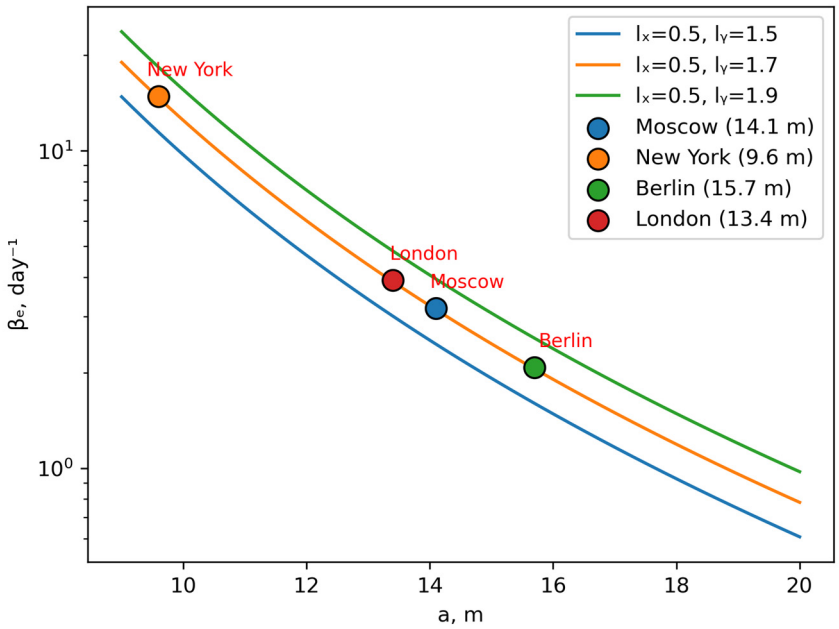

Figure 3. Comparison of the theoretical dependence and empirical data for various l_x and l_y values at $U_{tr} = 1$ m/s (here, l_x and l_y are measured in meters).

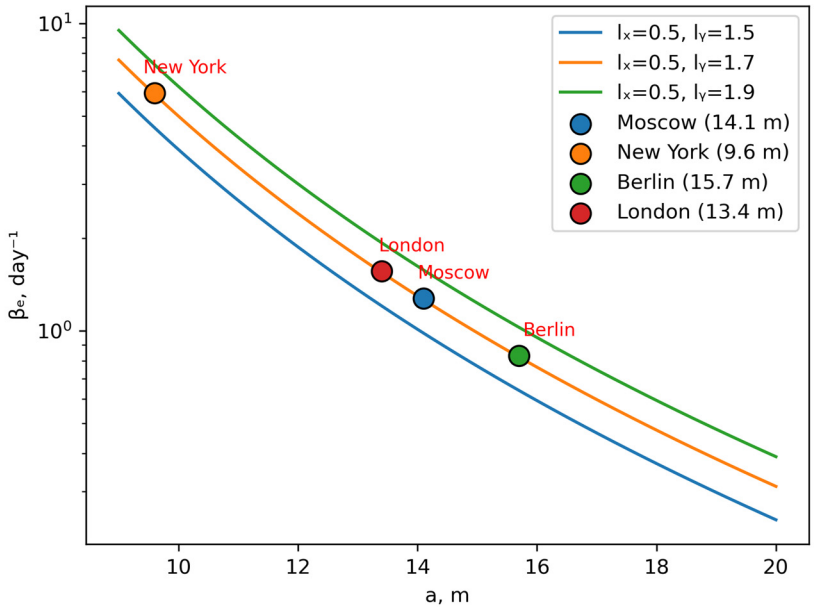

Figure 4. Comparison of the theoretical dependence and empirical data for various l_x and l_y values at $U_{tr} = 0.4$ m/s (here, l_x and l_y are measured in meters).

5. Social Mechanism of Infection Transmission

Now, we will consider the pure social mechanism of infection transmission when there is no relative movement of people. For example, such a situation is typical for groups of people confined to a limited space. In the case under consideration, $\zeta_I = 1$ and $\xi_I = 0$, the expression (6) is reduced to the following:

$$\beta_I = \nu_{sc} w = \nu_{sc} \left[1 - exp\left(-\frac{l_x l_y^2}{a^3} \right) \right], \tag{15}$$

A rough estimate of ν_{sc} can be performed based on the statistical data for the number of contacts that a person has during the day. According to [36–39], a person has $10 \leq k \leq 15$ daily contacts during an active period about of $4 \leq \Delta t \leq 8$ h, which is $14{,}400 \leq \Delta t \leq 28{,}800$ s. In this case, the active period is considered as the time during which a person meets other people, for example, during a working day. Therefore, the duration of one contact is $\tau_{sc} = \Delta t / k$, and the frequency of social contacts $\nu_{sc} = 1/\tau_{sc} = k/\Delta t$ lies in the interval $3{\cdot}10^{-4} \leq \nu_{sc} \leq 10^{-3}$ s^{-1}.

The corresponding dependencies of β_I on the distance between people for the limit values of Δt and k for the permissible l_x and l_y are shown in Figure 5. As is seen from these graphs, one may pay no regard to the spread of infection through the mechanism of social contacts at distances between people exceeding three meters due to the smallness of the β_I for $a \geq 3$ m.

Moreover, from graphs presented in Figures 2 and 5, it is seen that the value of β_I is at least four orders of magnitude smaller than the corresponding value of the β_E due to the smallness of the frequency ν_{sc}. Therefore, when $U_{tr} \neq 0$, the spread of infection always occurs through the transport mechanism. Herein, the social contact mechanism should be regarded as a limiting case of the transport mechanism as $U_{tr} \to 0$.

From the graphs presented in Figure 5, it is seen that the significant decrease in the value of β_I begins at a distance of one and a half meters. This corresponds to the widely accepted recommendations for maintaining social distance during the COVID-19 pandemic [40]. From this distance, there is a noticeable reduction in contact intensity, indicating a lower risk of infection and highlighting the importance of adhering to this guideline.

Finally, it should be noted that at large distances, a, both the constants β_E and β_I will take on negligibly small values matching in the order of magnitude. In this case, for some

l_x and l_y values, it is impossible to separate the infection transfer mechanisms. Such a peculiarity is of great interest since the external conditions determining the values of l_x and l_y can vary over a wide range. Moreover, the value of a can be changed locally, for example, in urban transport throughout the day. As a result, within a relatively short period, the constants β_E and β_I may be changed, which in principle can lead to the implementation of entirely different mechanisms of infection transmission. Consequently, the dynamics of establishing equilibrium in the system under consideration may come about in completely different ways.

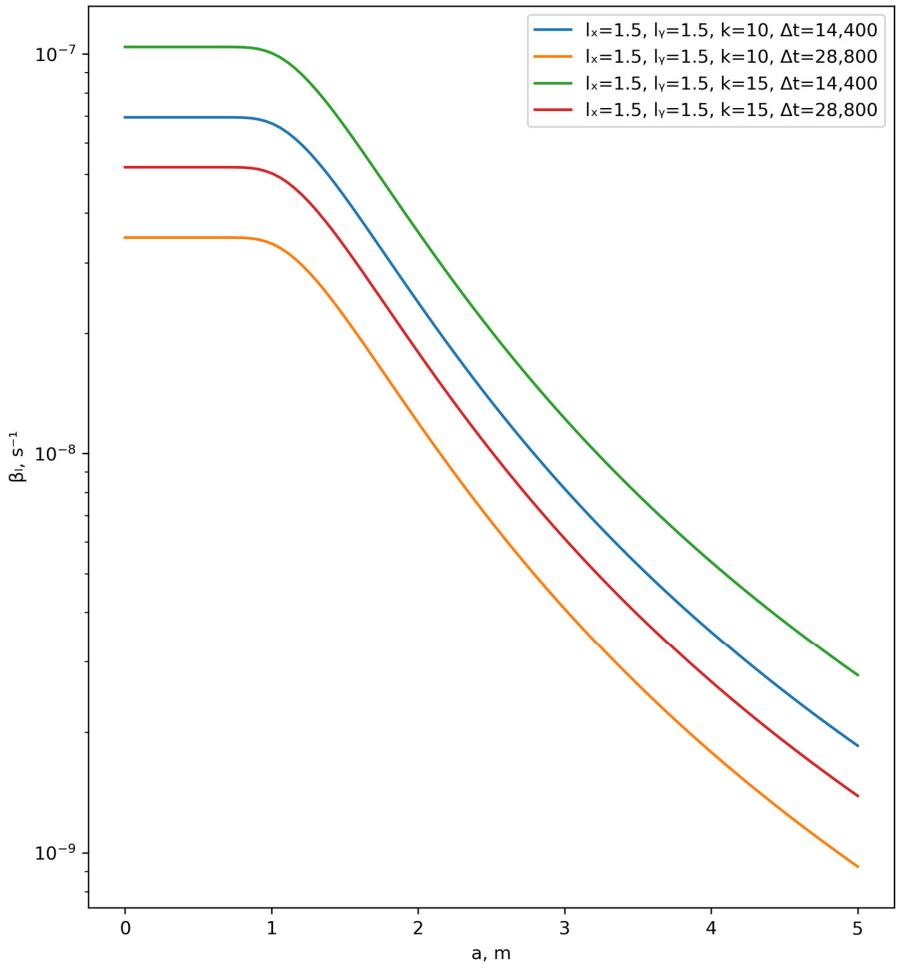

Figure 5. Dependence of β_I on the average distance between people a ($1 \leq a \leq 2$ m) for different Δt and k (here, l_x and l_y are measured in meters).

6. Dynamics near Endemic Equilibrium

In order to demonstrate these features, we examined the evolution of the system under consideration within the range of the parameters β_E and β_I, where one may compare the present results with those of the standard SEIR model. Herein, in all computations, we used $\varkappa = 0.14$ day^{-1}, which corresponds to an average incubation period of 7 days, $\gamma = 0.196$ day^{-1}, which corresponds to an average infectious period of 5.1 days and $\delta = 0.1$ day^{-1}, which corresponds to an average incubation time of 10 days. That is, as an illustration, we considered the case when the rate of transition to the healthy group is slightly higher than the rate of transition to the sick group. As the typical parameters of the considered population, we take that when l_x = 1 m and l_y = 0.5 m with $a = 1.5$ m and $U_{tr} = 1\ m/c$, the frequency of social contacts is $\nu_{sc} = 10^{-3}$ s^{-1}.

It was assumed that at the initial moment, there was a certain number of infection carriers and patients present in the population. All calculations were performed with the same initial data: $S_0 = 0.98$ and $E_0 = I_0 = 0.01$.

Figure 6 illustrates how the infection spreads solely through the transport mechanism. This script physically corresponds to an urban environment with intensive transportation flows, where all infected individuals of the I type are isolated. As is seen from the presented graphs, starting from day 20, the system reaches the endemic equilibrium when the majority of persons remains healthy. Herein, the number of infected and sick persons experiences significant growth during the same period.

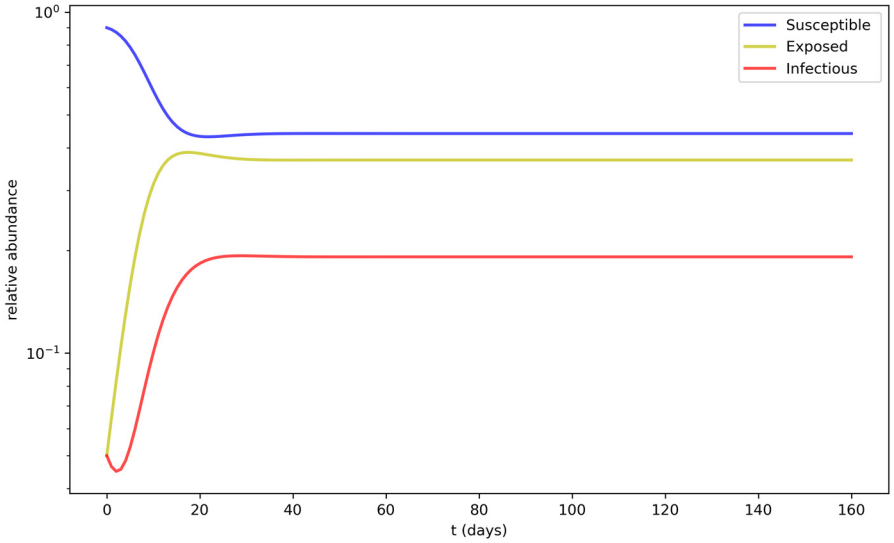

Figure 6. Evolution of the relative numbers of healthy, infected, and sick individuals with $\beta_E = 0.6$ day^{-1} and $\beta_I = 0$ day^{-1}.

A completely different dynamic is observed when only social contacts are considered. The typical result for this case is shown in Figure 7. There is a significant linear decrease in the number of infected and sick persons up to day 110, after which their quantity practically approaches zero. Meanwhile, the number of healthy persons tends towards the total relative population. This means that within the framework of the current model, the primary channel for the spread of the infection and the level of those infected and carriers of the infection are associated with the transport mechanism.

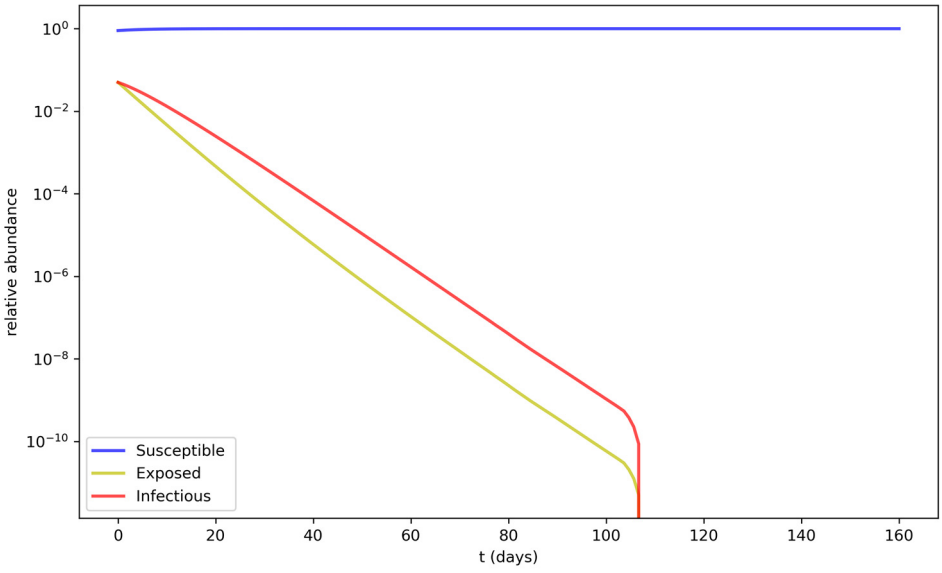

Figure 7. Evolution of the relative numbers of healthy, infected, and sick individuals with $\beta_E = 0$ day^{-1} and $\beta_I = 0.003$ day^{-1}.

It should be noted that under the combined influence of transportation and social infection mechanisms, the dynamics of reaching equilibrium (see Figure 8) are overall similar to the script of the perfect transportation mechanism, presented in Figure 6. However, in this case, the equilibrium level of latent persons (for t > 20 days) exceeds the proportion of healthy persons, as seen by comparing the curves presented in Figures 6 and 8. This script indicates a significant level of infectivity and rapid disease spread. As is seen from the provided graphs, the negligible frequency of social contacts in the case of the transportation-based spread mechanism is the factor that leads to the predominance of the latent category over the number of healthy people. Although, in this case, the proportion of sick persons remains at a sufficiently high level.

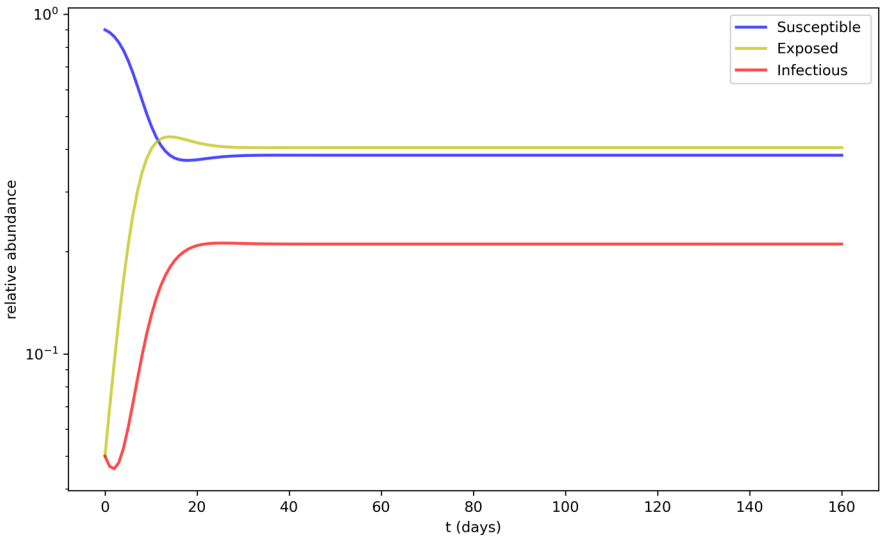

Figure 8. Evolution of the relative numbers of healthy, infected, and sick individuals with $\beta_E = 0.6$ day^{-1} and $\beta_I = 0.003$ day^{-1}.

7. Analysis of Endemic Equilibria

As is seen from these numerical examples, an endemic equilibrium is established in the system for a relatively short time, approximately $\tau_* \sim 20$ days. In fact, here we observe an equilibrium state where we have the following:

$$\frac{dS}{dt} = \frac{dE}{dt} = \frac{dI}{dt} = 0. \tag{16}$$

Proceeding from these conditions, in the system of (1)–(3), we obtain the following quasi-equilibrium state:

$$S_* = \frac{(\alpha+\delta)\gamma}{\beta_I\delta + \beta_E\gamma}, \quad I_* = \frac{\delta}{\delta+\gamma}\left[1 - \frac{\gamma(\delta+\alpha)}{\beta_I\delta+\beta_E\gamma}\right], \quad E_* = \frac{\gamma}{\delta+\gamma}\left[1 - \frac{\gamma(\delta+\alpha)}{\beta_I\delta+\beta_E\gamma}\right], \tag{17}$$

to which the system under consideration converges over the time period of $\tau_* = \tau_*(\beta_E)$. Noting that as β_E and the initial infection in the population, determined by the values E_0 and I_0, increase, the characteristic time to reach an endemic equilibrium τ_* decreases, and the ratio between the latent and infected individuals according to Equation (17) is established in the proportion $I_*/E_* = \delta/\gamma$. Since the relations in Equation (17) are meaningful only when $I_* \geq 0$ and $E_* \geq 0$, the following inequality must hold among the epidemiological constants:

$$\beta_I\delta + \beta_E\gamma > \gamma(\delta+\alpha). \tag{18}$$

This relationship should be interpreted as a necessary constraint imposed on the epidemiological constants by the condition for achieving an endemic equilibrium.

In this regard, there arises a natural question about the stability of the quasi-equilibrium state (17) with respect to the basic epidemiological constants [41]. In order to clarify this point, we tried to construct the corresponding Lyapunov [42] function for the system of (1)–(3). First, using (4), we eliminated S from the consideration by rewriting Equation (2) as follows:

$$\frac{dE}{dt} = E[\beta_E(1-E-I) - \delta - \alpha] + \beta_I I(1-E-I). \tag{19}$$

As a result, instead of the model of (1)–(3), we studied the system of (3) and (19), which with the help of relation (17), it is convenient to rewrite in a more illustrative form (see Appendix A) as follows:

$$\frac{dE}{dt} = E[a_1(E-E_*) + a_2(I-I_*)] + I[a_3(E-E_*) + a_4(I-I_*)], \tag{20}$$

$$\frac{dI}{dt} = \delta(E-E_*) + \gamma(I-I_*), \tag{21}$$

where

$$a_1 = -\beta_E,\ a_2 = -\frac{\beta_E E_* - \beta_I(1-E_*-I_*)}{E_*},\ a_3 = -\frac{\beta_I(1-I_*)}{E_*},\ a_4 = -\beta_I. \tag{22}$$

Let us pass over to construct the Lyapunov function for the system of (20) and (21). Define the function as follows:

$$V(E,I) = a\left(E - E_* - E_* \ln\frac{E}{E_*}\right) + b\left(I - I_* - I_* \ln\frac{I}{I_*}\right), \tag{23}$$

where a and b are some constants that have provided the asymptotic stability of (20) and (21) if there is as follows:

$$\frac{dV}{dt} < 0 \tag{24}$$

along the trajectory of the system of (20) and (21), as well as the following:

$$V(E,I) \geq 0 \tag{25}$$

for $E > 0$ and $I > 0$.

It is easy to see that the condition (25) is satisfied for any $a > 0$ and $b > 0$. Indeed, this can be verified by examining the behavior of the following function:

$$y(x) = x - x_* - x_* \ln\frac{x}{x_*} \tag{26}$$

whose derivative is as follows:

$$\frac{dy}{dx} = 1 - \frac{x_*}{x}. \tag{27}$$

From Equations (26) and (27), it follows that for $x < x_*$ we have the decreasing, positive function $y(x)$, which at point $x = x_*$ reaches its minimum $y(x = x_*) = 0$, and for $x > x_*$, this function is the increasing, positive function. That is, $y(x)$ is a positive function for $x > 0$, which implies that it holds for Equation (25).

Taking into account the following partial derivatives:

$$\frac{dV}{dE} = a\frac{E-E_*}{E_*},\ \frac{dV}{dI} = b\frac{I-I_*}{I_*}, \tag{28}$$

we can calculate the derivative for dV/dt along the trajectory (20) and (21) as follows:

$$\frac{dV}{dt} = -\beta_E a(E-E_*)^2 - \beta_I b(I-I_*)^2 + \Lambda(a,b)(E-E_*)(I-I_*), \tag{29}$$

where

$$\Lambda(a,b) = \frac{a\beta_I(1-E_*-I_*) - aB_E E_* - b\beta_I(1-I_*)}{E_*}. \quad (30)$$

As is seen from (29), the derivative dV/dt shall always be negative if as follows:

$$\Lambda(a,b) = 0, \quad (31)$$

from which it follows,

$$b = \frac{a\beta_I(1-E_*-I_*) - \beta_E E_*}{\beta_I(1-I_*)}. \quad (32)$$

Since for $a > 0$, it must hold $b > 0$, then from Equation (32), we find the following:

$$\frac{\beta_I}{\beta_E} > \frac{E_*}{1-E_*-I_*} \quad (33)$$

which is a condition for the derivative dV/dt to be negative.

Thus, $dV/dt < 0$ always holds except at the equilibrium point (I_*, E_*), and according to the Lyapunov theorem [36], the present equilibrium state is asymptotically stable in the positive quadrant ($E > 0$ and $I > 0$). Herein, the relations (18) and (33) describe the admissible diapason of the system parameters when there should be an endemic equilibrium.

8. Discussion and Prospects

In the present paper, the standard epidemic mean-field model was modified [see Equations (1)–(3)] in order to take into account separately the transfer of infection from sick and infected persons. To reveal these peculiarities in the simplest way, we moved away from considering the population change and the effect of acquired immunity. As a result, the findings presented in this study should be regarded as a prerequisite for a more complete treatment for an SEIS model with the allowance for processes of birth and death [43–45].

Herein, we proceeded from the assumption that the infection transmission for each category of people comes about in different ways, and these processes are characterized by the different rates of infection transmission. Such behavior is caused by several factors of different physical, biological, and social natures. In particular, the latent sick persons often interact with other people during their movements while the number of contacts for sick persons are limited to their immediate surroundings. That is, we have two different mechanisms of the infection spread: purely transport and social mechanisms of infection transmission.

To assess the impact of these mechanisms, based on the physical–chemical analogy, we proposed relationships for the rate constants of relevant epidemiological transitions depending on the gas–kinetic parameters of aerosols, the average distance between people, as well as the frequency of social contacts. It was shown that the proposed dependencies are in acceptable agreement with existing empirical data on infection transmission rate constants.

This means that the relations in (13) and (15) can also be applied in other epidemiological models to describe transitions from endemic to epidemic situations and vice versa, depending on the environmental conditions. However, one should take into consideration the dependence of β_E and β_I on the parameters U_{tr}, a, l_x, and l_y since these values can change over time. Nevertheless, such changes typically occur slowly with respect to the entire population under study by making the used approximation permissible. Of course, to consistently study these processes, the model of (1)–(3) would need to be supplemented with relations of the form $a = a(\mathrm{t})$, $l_x = l_x(t)$, and $l_y = l_y(\mathrm{t})$, but such an issue is beyond the framework of the present paper. At the same time, we showed that for $U_{tr} \neq 0$, the spread of infection always occurs through the transport mechanism, and the social contact mechanism should be regarded as a limiting case of the transport mechanism when $U_{tr} \to 0$.

In particular, these epidemiological constants β_E and β_I were used to examine the formation of endemic equilibria in the system under consideration. Such equilibria can arise as a non-trivial stationary distribution [see Equation (17)] when balance is achieved between the sick and the recovered, requiring consideration of the latent phase of the disease, during which an individual is already a virus carrier but not yet sick. It is this moment that is of considerable practical interest, since in the present case, one can observe the disease in the population for any length of time. Employing the method of the Lyapunov function, we found the range of the system parameters [see Equations (18) and (33)] where there may exist such endemic states.

Finally, we again would like to emphasize that one major difference between SEIR and SEIS models is the formation of corresponding quasi-equilibrium states. Therefore, it would be interesting to qualitatively compare the predicted epidemiological dynamics of both models under identical initial conditions.

To perform this comparation, we considered the standard SEIR model written for the constant population size:

$$\frac{dS}{dt} = -\beta SI, \tag{34}$$

$$\frac{dE}{dt} = \beta SI - \delta E, \tag{35}$$

$$\frac{dI}{dt} = \delta E - \gamma I, \tag{36}$$

$$\frac{dR}{dt} = \gamma I, \tag{37}$$

where R is the proportion of the recovered persons who have developed immunity to the specific disease (it is worth noting that this may be a permanent or temporary acquired immunity). In this case, we set $\beta = \beta_E + \beta_I$; herein, all other constants and initial conditions were taken as in the calculations shown in Figure 8.

Figure 9 illustrates what typically happens to the system under consideration based on the SEIR model. From the comparison of similar dependencies presented in Figures 8 and 9, it is seen that these models fundamentally describe different physical limits: in the SEIR model, complete recovery of the population ($S_* \to 1$) inevitably occurs due to inherent immunity, while in the SEIS case, an endemic equilibrium (17) is reached.

However, as is seen from (17) that in the following case:

$$\frac{\gamma(\delta + \alpha)}{\beta_I \delta + \beta_E \gamma} = 1 \tag{38}$$

it holds that $S_* \to 1$ under $t \to \infty$ as in the SEIR model. In particular, for simplicity, by setting $\beta_I = 0$, we obtain $\beta_E = \delta + \alpha = 0.24$. The dependencies presented in Figure 10 clearly illustrate the dynamics of this case.

In contrast to the SEIR model, where peaks of infection carriers are observed (Figure 9), for the SEIS model, there is a monotonic recovery of the population from the initial state to $S_* = 1$ by eliminating the infection within the population ($I_* = E_* = 0$). It should be noted that the limit described in Equation (38) is not a difficult-to-realize case. Considering the dependence of β_E and β_I on the system parameters, where these epidemiological constants vary widely (see Figures 2 and 5), one can always expect a transition from the script presented in Figure 8 to the case depicted in Figure 10.

Moreover, one can try to govern this process by changing the frequency of social contacts since there is a strong influence of population change and socio-cultural factors of people across the territory in the formation of an endemic equilibrium [46,47]. So, proceeding from the results based on the conception of the Nash equilibrium [48–50], one may expect completely different dynamics of the disease development depending on the type of socio-cultural behavior of the people. Perhaps, this point allows us to come to find the theoretical description for the epidemiological constants α, γ, and δ.

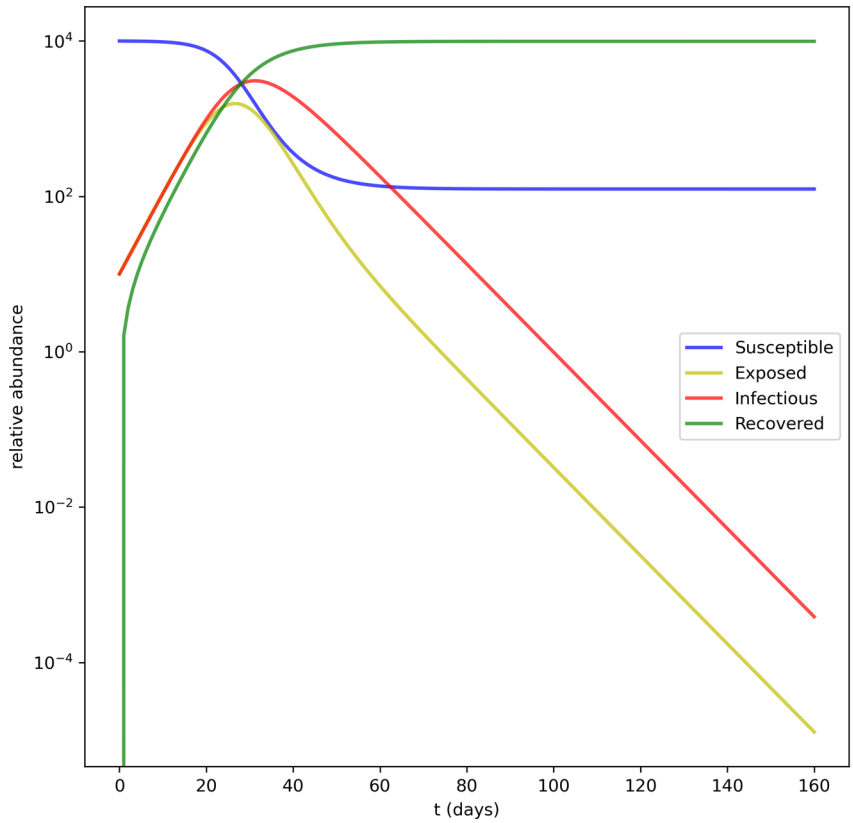

Figure 9. Evolution of the relative numbers of healthy, infected, sick, and recovered individuals in the SEIR model with $\beta = 0.6003$ day^{-1}.

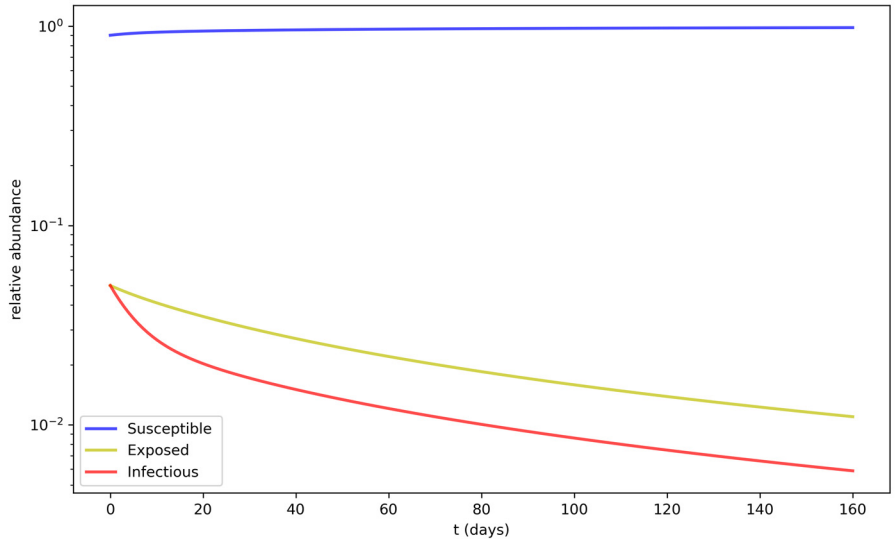

Figure 10. Evolution of the relative numbers of healthy, infected, and sick individuals with $\beta_E = 0.24$ day^{-1} and $\beta_I = 0$ day^{-1}.

Author Contributions: Conceptualization, A.R.K. and M.A.S.; methodology, A.R.K. and A.N.B.; validation, A.R.K., A.N.B. and M.A.S.; investigation, A.R.K., A.N.B. and M.A.S.; data curation, M.A.S.; writing—review and editing, A.R.K. and M.A.S.; supervision, A.R.K.; funding acquisition, A.R.K. All authors have read and agreed to the published version of the manuscript.

Funding: This work was supported by the Ministry of Science and Higher Education of the Russian Federation (State Assignment No. 075-00270-24-00).

Data Availability Statement: The original contributions presented in this study are included in the article. Further inquiries can be directed to the corresponding author.

Conflicts of Interest: The authors declare no conflicts of interest.

Appendix A

The purpose of this Appendix A is to obtain Equations (20)–(22). Rewrite Equation (19) as follows:

$$\frac{dE}{dt} = -\beta_E E^2 - \beta_I I^2 - (\beta_E + \beta_I)EI + (\beta_E - \delta - \alpha)E + \beta_I I. \tag{A1}$$

On the other hand, Equation (19) should take the following form:

$$\frac{dE}{dt} = E[a_1(E - E_*) + a_2(I - I_*)] + [a_3(E - E_*) + a_4(I - I_*)], \tag{A2}$$

where a_1, a_2, a_3, a_4 are unknown constants to be determined, and E_* and I_* are defined by relation (17). Therefore, comparing the terms in (A1) and (A2) at corresponding degrees of E and I, we obtain the following:

$$a_1 = -\beta_E, \tag{A3}$$

$$a_4 = -\beta_I, \tag{A4}$$

$$a_2 + a_3 = -(\beta_I + \beta_E), \tag{A5}$$

$$E_* a_1 + I_* a_2 = \delta + \alpha - \beta_E\,, \tag{A6}$$

$$E_* a_3 + I_* a_4 = -\beta_I. \tag{A7}$$

Moreover, the values E_* and I_* satisfy the following equations:

$$\beta_E E_*^2 + \beta_I I_*^2 + (\beta_E + \beta_I)E_* I_* + (\alpha + \delta - \beta_E)E_* - \beta_I I_* = 0, \tag{A8}$$

$$\delta E_* - \gamma I_* = 0. \tag{A9}$$

From (A4) and (A7), we obtain the following:

$$a_3 = -\frac{\beta_I(1 - I_*)}{E_*}. \tag{A10}$$

Inserting (A10) into (A5), we obtain the following:

$$a_2 = \frac{\beta_I(1 - I_* - E_*) - \beta_E E_*}{E_*}. \tag{A11}$$

At the same time, the substitution of this value a_2 into (A6) turns this relation into an identity because of (A8).

Finally, subtracting (A9) from (3), we obtain the following:

$$\frac{dI}{dt} = \delta(E - E_*) - \gamma(I - I_*) \tag{A12}$$

as was shown.

References

1. Brauer, F.; Castillo-Chavez, C. *Mathematical Models in Population Biology and Epidemiology*, 2nd ed.; Springer: New York, NY, USA, 2012.
2. Hethcote, H.W. The mathematics of infectious diseases. *SIAM Rev.* **2000**, *42*, 599–653. [CrossRef]
3. He, S.; Peng, Y.; Sun, K. SEIR modeling of the COVID-19 and its dynamics. *Nonlinear Dyn.* **2020**, *101*, 1667–1680. [CrossRef] [PubMed]
4. Diekmann, O.; Heesterbeek, J. *Mathematical Epidemiology of Infectious Diseases: Model Building, Analysis and Interpretation*; John Wiley & Sons: New York, NY, USA, 2000.

5. Allen, L.J.S. An introduction to stochastic epidemic models. In *Mathematical Epidemiology*; Springer: Berlin/Heidelberg, Germany, 2008; Volume 3, pp. 81–130.
6. Avilov, K.K.; Romanyuha, A.A. Mathematical models of distribution and control tuberculosis. *Math. Biol. Bioinform.* **2007**, *22*, 188–318. [CrossRef]
7. Ojo, M.M.; Peter, O.J.; Goufo, E.F.D.; Panigoro, H.S.; Oguntolu, F.A. Mathematical model for control of tuberculosis epidemiology. *J. Appl. Math. Comput.* **2022**, *69*, 1865–2085. [CrossRef]
8. Lopez, A.D.; Mathers, C.D. Measuring the global burden of disease and epidemiological transitions: 2002–2030. *Ann. Trop. Med. Parasitol.* **2006**, *100*, 481–499. [CrossRef]
9. Mwalili, S.; Kimathi, M.; Ojiambo, V.; Gathungu, D.; Mbogo, R. SEIR model for COVID-19 dynamics incorporating the environment and social distancing. *BMC Res. Notes* **2020**, *13*, 352. [CrossRef]
10. Leonov, A.; Nagornov, O.; Tyuflin, S. Modeling of Mechanisms of Wave Formation for COVID-19 Epidemic. *Mathematics* **2023**, *11*, 167. [CrossRef]
11. Prigozhin, I.; Kondepudi, D. *Modern Thermodynamics: From Heat Engines to Dissipative Structures*; Mir: Moscow, Russia, 2002; pp. 319–425.
12. Kucharski, A.J.; Russell, T.W.; Diamond, C.; Liu, Y.; Edmunds, J.; Funk, S.; Eggo, R. Early dynamics of transmission and control of COVID-19: A mathematical modelling study. *Lancet Infect. Dis.* **2020**, *20*, 553–558. [CrossRef]
13. Lin, Q.; Zhao, S.; Gao, D.; Lou, Y.; Yang, S.; Musa, S.S.; Wang, M.H.; Cai, Y.; Wang, W.; Yang, L.; et al. A conceptual model for the outbreak of Coronavirus disease 2019 (COVID-19) in Wuhan, China with individual reaction and governmental action. *Int. J. Infect. Dis.* **2020**, *93*, 211–216. [CrossRef]
14. Brauer, F.; Castillo-Chavez, C.; Feng, Z. *Mathematical Models in Epidemiology*, 1st ed.; Springer: New York, NY, USA, 2019; Volume 69, 619p.
15. Tomchin, D.A.; Fradkov, A.L. Prediction of the COVID-19 spread in Russia based on SIR and SEIR models of epidemics. *Ifac-papersonline* **2020**, *53*, 833–838. [CrossRef]
16. Coburn, B.J.; Wagner, B.G.; Blower, S. Modeling influenza epidemics and pandemics: Insights into the future of swine flu (H1N1). *BMC Med.* **2009**, *7*, 30. [CrossRef] [PubMed]
17. Longini, I.M.; Nizam, A.; Xu, S.; Ungchusak, K.; Hanshaoworakul, W.; Cummings, D.A.T.; Halloran, M.E. Containing pandemic influenza at the source. *Science* **2005**, *309*, 1083–1087. [CrossRef] [PubMed]
18. Mossong, J.; Hens, N.; Jit, M.; Beutels, P.; Auranen, K.; Mikolajczyk, R.; Massari, M.; Salmaso, S.; Tomba, G.S.; Wallinga, J.; et al. Social contacts and mixing patterns relevant to the spread of infectious diseases. *PLoS Med.* **2008**, *5*, e74. [CrossRef]
19. Read, J.M.B., Jr.; Cummings, D.A.; Ho, A.; Jewell, C.P. Novel coronavirus 2019-nCoV: Early estimation of epidemiological parameters and epidemic predictions. *medRxiv* **2020**. [CrossRef]
20. Elie, R.; Hubert, E.; Turinici, G. Contact rate epidemic control of COVID-19: An equilibrium view. *arXiv* **2020**, arXiv:2004.08221. [CrossRef]
21. Shereen, M.A.; Khan, S.; Kazmi, A.; Bashir, N.; Siddique, R. COVID-19 infection: Origin, transmission, and characteristics of human coronaviruses. *J. Adv. Res.* **2020**, *24*, 91–98. [CrossRef]
22. Karimov, A.R.; Stenflo, L.; Yu, M.Y. Dynamics of charged aerosols relevant to transmission of airborne infections. *Phys. Scr.* **2022**, *97*, 085007. [CrossRef]
23. Karimov, A.R.; Solomatin, M.A. Peculiarities of aerosol particle propagation in technogenic conditions. *Bull. Natl. Res. Inst. MEPhI* **2024**, *13*, 30–39.
24. Virgo, S.E. Loschmidt's Number. In *Science Progress in the Twentieth Century*; Sage Publications, Ltd.: Thousand Oaks, CA, USA, 1933; Volume 27, pp. 34–649.
25. Liska, D.; Gritsev, V. The loschmidt index. *SciPost Phys.* **2021**, *10*, 100. [CrossRef]
26. Lauer, S.A.; Grantz, K.H.; Bi, Q.; Jones, F.K.; Zheng, Q.; Meredith, H.R.; Azman, A.S.; Reich, N.G.; Lessler, J. The incubation period of coronavirus disease 2019 (COVID-19) from publicly reported confirmed cases: Estimation and application. *Ann. Intern. Med.* **2020**, *172*, 577–582. [CrossRef]
27. Guan, W.-J.; Ni, Z.-Y.; Hu, Y.; Liang, W.-H.; Ou, C.-Q.; He, J.-X.; Liu, L.; Shan, H.; Lei, C.-L.; Hui, D.S. Clinical characteristics of coronavirus disease 2019 in China. *N. Engl. J. Med.* **2020**, *382*, 1708–1720. [CrossRef] [PubMed]
28. He, X.; Lau, E.H.Y.; Wu, P.; Deng, X.; Wang, J.; Hao, X.; Lau, Y.C.; Wong, J.Y.; Guan, Y.; Tan, X.; et al. Temporal dynamics in viral shedding and transmissibility of COVID-19. *Nat. Med.* **2020**, *26*, 672–675. [CrossRef] [PubMed]
29. Qin, J.; You, C.; Lin, Q.; Hu, T.; Yu, S.; Zhou, X.-H. Estimation of incubation period distribution of COVID-19 using disease onset forward time: A novel cross-sectional and forward follow-up study. *medRxiv* **2020**, *6*, eabc1202. [CrossRef] [PubMed]
30. Tudor-Locke, C.; Craig, C.L.; Beets, M.W.; Belton, S.; Cardon, G.M.; Duncan, S.; Hatano, Y.; Lubans, D.R.; Olds, T.S.; Raustorp, A.; et al. How many steps/day are enough? for children and adolescents. *Int. J. Behav. Nutr. Phys. Act.* **2011**, *8*, 78. [CrossRef]
31. Ali, M.; Shah, S.T.H.; Imran, M.; Khan, A. The role of asymptomatic class, quarantine and isolation in the transmission of COVID-19. *J. Biol. Dyn.* **2020**, *14*, 389–408. [CrossRef]
32. Ferguson, N.; Laydon, D.; Nedjati-Gilani, G.; Imai, N.; Ainslie, K.; Baguelin, M. Imperial College COVID-19 Response Team. In *Impact of Nonpharmaceutical Interventions (NPIs) to Reduce COVID19 Mortality and Healthcare Demand*; Imperial College: London, UK, 2020; pp. 1–20.

33. Kudryashov, N.A.; Rybka, R.B.; Sboev, A.G.; Serenko, A.V. Parameters of the SIR Model for the First and Second Waves of Coronavirus in Moscow. *Bull. Natl. Res. Nucl. Univ. MEPhI* **2023**, *6*, 561–566.
34. Flaxman, S.; Mishra, S.; Gandy, A.; Unwin, H.J.T.; Mellan, T.A.; Coupland, H.; Whittaker, C.; Zhu, H.; Berah, T.; Eaton, J.W.; et al. Estimating the effects of non-pharmaceutical interventions on COVID-19 in Europe. *Nature* **2020**, *584*, 257–261. [CrossRef]
35. Galeeva, J.S.; Fedorov, D.E.; Starikova, E.V.; Manolov, A.I.; Pavlenko, A.V.; Selezneva, O.V.; Klimina, K.M.; Veselovsky, V.A.; Morozov, M.D.; Yanushevich, O.O.; et al. Microbial signatures in COVID-19: Distinguishing mild and severe disease via gut microbiota. *Biomedicines* **2024**, *12*, 996. [CrossRef]
36. Arenas, A.; Cota, W.; Gómez-Gardeñes, J.; Gómez, S.; Granell, C.; Matamalas, J.T.; Soriano-Paños, D.; Steinegger, B. Modeling the Spatiotemporal Epidemic Spreading of COVID-19 and the Impact of Mobility and Social Distancing Interventions. *Phys. Rev. X* **2020**, *10*, 041055. [CrossRef]
37. Schönrath, K.; Klein-Szanto, A.J.; Braunewell, K.H. The putative tumor suppressor VILIP-1 counteracts epidermal growth factor-induced epidermal-mesenchymal transition in squamous carcinoma cells. *PLoS ONE* **2012**, *7*, e33116. [CrossRef]
38. Read, J.M.; Lessler, J.; Riley, S.; Wang, S.; Tan, L.J.; Kwok, K.O.; Guan, Y.; Jiang, C.Q.; Cummings, D.A.T. Social mixing patterns in rural and urban areas of southern China. *Proc. R. Soc. B Biol. Sci.* **2014**, *281*, 20140268. [CrossRef] [PubMed]
39. Eubank, S.; Guclu, H.; Anil Kumar, V.S.; Marathe, M.V.; Srinivasan, A.; Toroczkai, Z.; Wang, N. Modelling disease outbreaks in realistic urban social networks. *Nature* **2004**, *429*, 180. [CrossRef] [PubMed]
40. Fong, M.W.; Gao, H.; Wong, J.Y.; Xiao, J.; Shiu, E.Y.C.; Ryu, S.; Cowling, B.J. Nonpharmaceutical measures for pandemic influenza in nonhealthcare settings—Social distancing measures. *Emerg. Infect. Dis.* **2020**, *5*, 976. [CrossRef] [PubMed]
41. Kudryashov, N.A.; Chmykhov, M.A.; Vigdorowitsch, M. Analytical Features of the SIR Model and their Applications to COVID-19. *Appl. Math. Model.* **2021**, *90*, 466–473. [CrossRef]
42. Lyapunov, A.M. The general problem of the stability of motion. *Int. J. Control.* **1992**, *55*, 531–534. [CrossRef]
43. Harko, T.; Lobo, F.S.N.; Mak, M.K. Exact analytical solutions of the susceptible-infected-recovered (SIR) epidemic model and of the SIR model with equal death and birth rates. *Appl. Math. Comput.* **2014**, *236*, 184–194. [CrossRef]
44. Kuhnert, D.; Stadler, T.; Vaughan, T.G.; Drummond, A.J. Simultaneous reconstruction of evolutionary history and epidemiological dynamics from viral sequences with the birth-death SIR model. *J. R. Soc. Interface* **2014**, *11*, 20131106. [CrossRef]
45. Allen, L.J. Some discrete-time SI, SIR, and SIS epidemic models. *Math. Biosci.* **1994**, *124*, 83–105. [CrossRef]
46. Markovic, R.; Šterk, M.; Marhl, M.; Perc, M.; Gosak, M. Socio-demographic and health factors drive the epidemic progression and should guide vaccination strategies for best COVID-19 containment. *Results Phys.* **2021**, *26*, 104433. [CrossRef]
47. Demina, M.V.; Kudryashov, N.A. Polynomial method for constructing equilibrium configurations of point vortices in the plane. *Model. Anal. Inf. Syst.* **2015**, *19*, 50–55. [CrossRef]
48. Laguzet, L.; Turinici, G. Individual vaccination as Nash equilibrium in a SIR model with application to the 2009–2010 influenza A (H1N1) epidemic in France. *Bull. Math. Biol.* **2015**, *77*, 1955–1984. [CrossRef] [PubMed]
49. Nash, J.F. Equilibrium points in n-person games. *Proc. Natl. Acad. Sci. USA* **1950**, *36*, 48–49. [CrossRef] [PubMed]
50. Perisic, A.; Bauch, C.T. Social contact networks and disease eradicability under voluntary vaccination. *PLoS Comput. Biol.* **2009**, *5*, e1000280. [CrossRef] [PubMed]